

# Control Strategy for Power Generation from a Capacitive Mixing Cell and Grid Injection

Armel A. Nkembí<sup>1</sup>, Alberto M. Pernía<sup>1</sup>, Miguel J. Prieto<sup>1</sup>, Ana Arenillas<sup>2</sup> and J. R. Álvarez<sup>3</sup>

<sup>1</sup> Department of Electrical Engineering  
Universidad de Oviedo

Campus Universitario, EDO 3 – 33203 Gijón (Spain)

Phone number:+0034 985 182566, e-mail: [uo278913@uniovi.es](mailto:uo278913@uniovi.es), [amartinp@uniovi.es](mailto:amartinp@uniovi.es), [mike@uniovi.es](mailto:mike@uniovi.es)

<sup>2</sup> Instituto de Ciencia y Tecnología del Carbono (INCAR-CSIC)  
c/ Francisco Pintado Fe, 26 – 33011 Oviedo (Spain)

Phone number:+0034 985 119090, e-mail: [aapunte@incar.csic.es](mailto:aapunte@incar.csic.es)

<sup>3</sup> Department of Chemical Engineering and Environmental Technology  
Universidad de Oviedo

C/Julián Clavería, 8 – 33006 Oviedo (Spain)

Phone number:+0034 985 103028, e-mail: [jras@uniovi.es](mailto:jras@uniovi.es)

**Abstract.** In this work, the possibility of extracting energy from a capacitive mixing cell based on the potential that exists as a result of the salinity gradient between fresh and salt water passing through the electrodes of a deionization cell is studied. For this, a two-stage process is defined. The first step uses a dual buck-boost converter for the positive and negative cycles of the input voltage. This topology acts as a current source and is chosen due to its ability to provide high power factor and to work with extremely low voltage levels. The second stage consists of an H-bridge inverter synchronized with the AC grid to feed power into the grid. A hysteresis control system has been designed for the current flowing through the coil. With this, it has been analyzed how the efficiency of the total system (cell + power converter) varies with the changes in the series resistance of the CapMix cell or with the discharge current selected in the power converter. Simulations are carried out to characterize the energy extraction and some experimental results confirm the possibility of using this new renewable energy source.

**Key words.** CapMix cell, Capacitive Donnan Potential (CDP), low voltage energy harvesting, buck/boost converter, hysteresis control.

## 1. Introduction

Energy is a necessary component for the advancement of human civilization. Fossil fuels supply more than 73.5% of the world's electricity production [1], but their use results in excess greenhouse gases in the atmosphere, especially carbon dioxide. The most environmentally friendly solution would be to use renewable energy sources such as solar, wind, hydroelectric, ocean or biomass. Another form of renewable energy to consider is blue energy (or salinity difference energy), which uses the energy released when two solutions of different salinity concentrations are

combined, which occurs constantly in river bodies [2]. This mixing energy is considered renewable, as fresh water is replenished by the global hydrological cycle.

In recent decades, research has been carried out to find efficient methods of harvesting salinity gradient energy. Among them, membrane-based techniques are the most advanced: Pressure Retarded Osmosis (PRO) and Reverse Electrodialysis (RED) [3]. PRO generates an osmotic pressure difference between two chambers to produce pressurized water that allows electricity to be generated by means of a hydraulic turbine. RED creates an electrical potential difference between the electrodes of a cell where dilute and concentrated solutions flow separated by cation and anion exchange membranes alternately [4]. At the moment, these methods are used only on a laboratory scale. In addition, they have certain limitations that must be resolved before they can be commercialized, the most important being the efficiency and cost of the membranes in the case of RED, and the need to use electromechanical converters such as dynamos or turbines in PRO [5].

An alternative to the aforementioned techniques is called CapMix (Capacitive Mixing), which is based on the variation of the potential difference that appears between two nanoporous electrodes due to the exchange of the ionic content of the solution between them. There are three main CapMix techniques: CDLE (Capacitive Double Layer Expansion), CDP (Capacitive Donnan Potential), and MEB (Mixed Entropy Battery, which combines aspects of CDLE and CDP). In CDLE, the electrodes are charged by an external power supply, while CDP incorporates permeability-selective membranes that allow only one type of ion (cation or anion) to flow through them

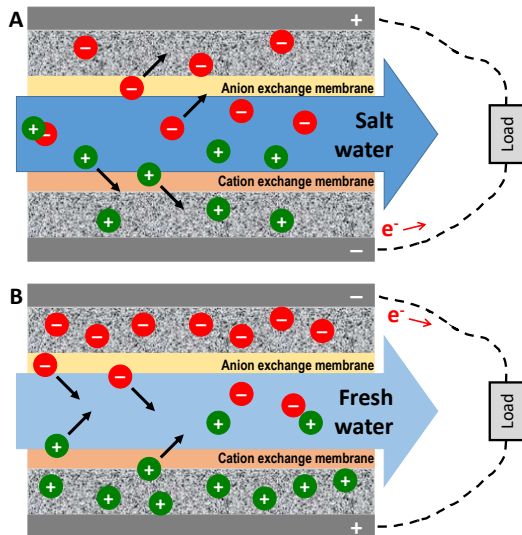


Fig. 1 (A) Loading of the CapMix cell with a concentrated solution. (B) CapMix cell discharge with a diluted solution.

[6]. MEB, on the other hand, uses reactive electrodes (instead of inert electrodes, as in CDLE and CDP) to extract the blue energy stored in these electrodes in the form of chemical energy. The CapMix cell used in this work uses the CDP principle.

The operating principle of the CapMix cell based on the Donnan potential (CDP) is illustrated in Fig. 1. When a concentrated solution (such as seawater) passes through the cell, the ions leave the solution and pass into the electrodes through the exchange membranes. As a result of this diffusion process, placing an external load will make electrons circulate from one electrode to the other, (Fig. 1A). In the discharge process, a dilute solution (such as river water) passes through the cell and the ions initially deposited on the electrodes flow through the ion-selective membranes into solution; the electrodes are discharged and the electrons circulate in the opposite direction through the external load (Fig. 1B) [3]. Thus, by alternating the flow of freshwater and saltwater in the spacer channel, continuous energy production is generated as illustrated in Fig. 2.

The three techniques mentioned (PRO, RED and CapMix) are inverse processes of desalination processes: reverse osmosis, electrodialysis and capacitive deionization, respectively. Instead of consuming energy to desalinate salty streams, the reverse operation is used to produce energy by mixing solutions in different concentrations.

The two main obstacles to using blue energy are: finding ideal locations with salinity difference and developing appropriate strategies for converting blue energy into a useful electrical form. This last point is the object of this work. A high-gain boost converter collects the energy from the capacitive cell and delivers it to an AC network.

The rest of this work is organized as follows: Section 2 discusses the characterization of the electrodes used to build the cell. Section 3 shows how to measure the electrical parameters of the cell. Section 4 collects the operation of the proposed converter to transfer the energy to the mains.

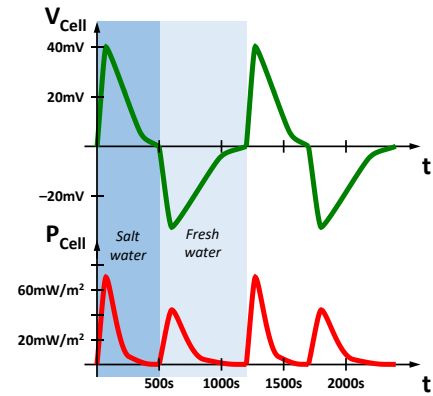


Fig. 2 Voltage and power production in a CDP CapMix cell.

Section 5 shows some simulations carried out with PLECS that allow analyzing the efficiency of the system. Section 6 contains the results obtained with a prototype, and Section 7 contains the conclusions.

## 2. Characteristics of the Electrodes

The electrodes of the CapMix cell must be capable of adsorbing as many ions as possible that pass through the selective exchange membranes and are deposited on them. For this to happen, they need to have as much surface area as possible to increase their capacity. The CapMix cell electrode current collector must be covered with activated carbon deposits, which has a high specific surface area [7] and allows the maximum exchange of charges.

The voltage across the electrodes each charge and discharge cycle is about 100mV. To increase the energy that can be extracted from the CapMix cells, they are stacked together in series-parallel configurations (Fig. 3) and the distance between the electrodes is optimized.

## 3. Measurement of the Cell Parameters

The electrical connection of the electrodes creates an equivalent that behaves like a supercapacitor. These devices benefit from their electrical double-layer structure and are increasingly used in power electronics, with precise and well-validated models [8]. The model used in

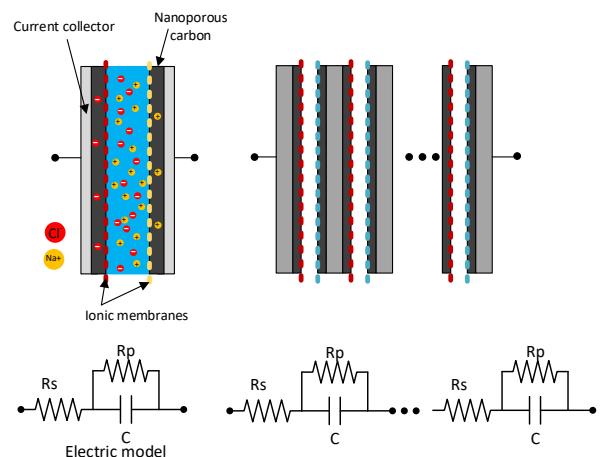


Fig.3 Activated carbon electrodes connected in series.

this work is the one shown in Fig. 3, which has three parameters: a capacitor (C), an equivalent series resistance (Rs) that represents ohmic losses, and a parallel resistance (Rp) that represents losses due to leakage current. To determine the value of these parameters in the case of the CapMix cell, we pass saline water of a given concentration to an initially clean cell [8]. The cell terminals are then connected to a current source that charges the cell to a maximum voltage of 1V to prevent electrolysis of the water. As the cell charges at constant current, ions continually deposit on the electrodes, charging capacitor C. When the cell is switched off, self-discharge occurs. The total charge-discharge process is shown in Fig. 4, in which the value of Rs can be determined by measuring the cell voltage at the point where the charging process begins and applying Ohm's law:

$$R_s = \frac{V_1}{I} \quad (1)$$

During the charging process, assuming approximately linear behavior, the cell voltage is given by equation (2), from which the capacity C can be obtained:

$$V_2 - V_1 \approx \frac{I}{C} \cdot (t_2 - t_1) \quad (2)$$

During the cell self-discharge, the voltage evolution is approximately given by equation (3).

$$V_{in} \approx V_3 \cdot \exp \left[ - \left( \frac{t-t_2}{R_p C} \right) \right] \quad (3)$$

Selecting any two points on the cell discharge curve [(t<sub>p1</sub>, V<sub>p1</sub>) and (t<sub>p2</sub>, V<sub>p2</sub>)] and using equation (3), the leakage resistance can be calculated as:

$$R_p = - \frac{t_{p1} - t_{p2}}{C \cdot \ln \left( \frac{V_{p1}}{V_{p2}} \right)} \quad (4)$$

The value of these parameters depends on the concentration of the solution that passes through the electrodes (M), on the surface of the solution in contact with the electrodes (S), on the distance between the electrodes (d) and on the number of electrodes connected in series (n) and in parallel (m). All this defines the maximum energy that can be extracted from the CapMix cell.

Table I lists the cell parameters for a particular concentration of solution (M) between the electrodes and

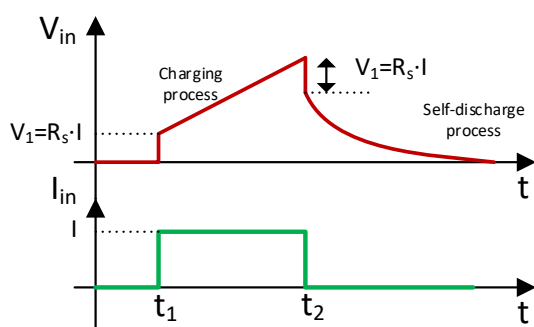


Fig. 4 Variation of the voltage in the CapMix cell during its charge and discharge.

considering different contact surfaces (S). The solutions used have been prepared by dissolving a certain amount of NaCl salt in a volume of water.

Table I. - Parameters of Capmix Cells

S [mm <sup>2</sup> x 170]	M [g/l]	R <sub>s</sub> [mΩ]	R <sub>p</sub> [Ω]	C [F]
50	12	75	23.68	6.50
100		55	12.13	13.00
150		37.5	8.68	21.55
200		17.5	7.85	27.91
50	24	45	26.45	10.53
100		30	18.75	18.83
150		15	14.80	27.56
200		12.5	9.68	34.43
50	36	30	27.55	10.80
100		20	24.00	20.99
150		12.5	16.78	30.00
200		7.5	11.39	37.83

The cell parameters shown in Table I were obtained using a laboratory prototype composed of two graphite electrodes separated by a distance (d) of 2mm.

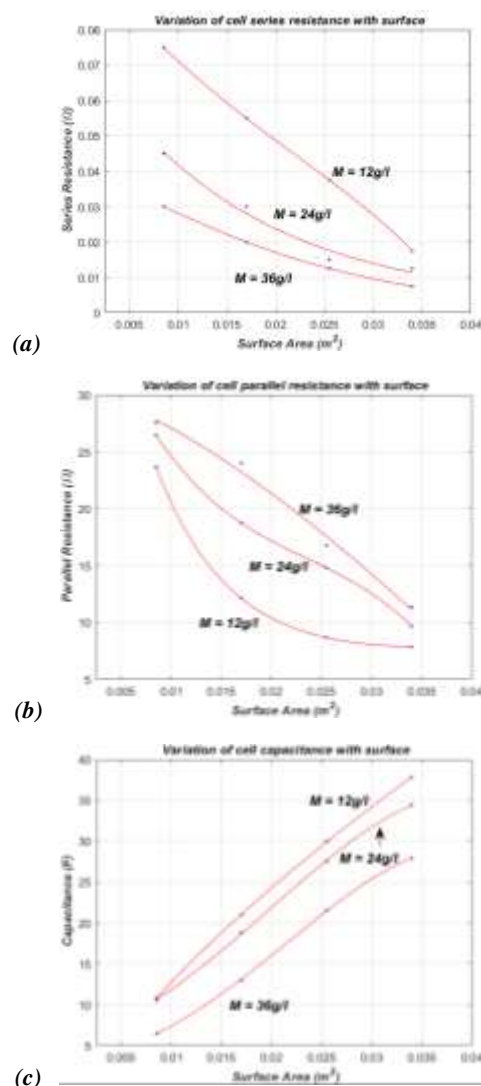


Fig. 5 Variation of the parameters of a cell as a function of the surface for different concentrations of salt. (a) Series resistance. (b) Parallel resistance. (c) Capacity.

To calculate the optimal energy that can be derived from a cell of this type, it is necessary to obtain approximate mathematical models that describe the information shown in Table I. Fig. 5 represents these data in the form of fitted curves with MATLAB. From the curves in Fig. 5a:

$$R_s(S)|_{M=\frac{12g}{l}} = -2,463 \cdot 10^{-4} \cdot e^{120,2 \cdot S} + 0,1007 \cdot e^{-33,56 \cdot S} \quad (5)$$

$$R_s(S)|_{M=\frac{24g}{l}} = 0,07328 \cdot e^{-59,33 \cdot S} + 0,001097 \cdot e^{11,63 \cdot S} \quad (6)$$

$$R_s(S)|_{M=\frac{36g}{l}} = 0,049 \cdot e^{-54,46 \cdot S} \quad (7)$$

From Fig. 5b, we obtain equations for Rp:

$$R_p(S)|_{M=\frac{12g}{l}} = 54,59 \cdot e^{-133,5 \cdot S} + 5,79 \cdot e^{6,683 \cdot S} \quad (8)$$

$$R_p(S)|_{M=\frac{24g}{l}} = -1,335 \cdot 10^6 \cdot S^3 + 9,405 \cdot 10^4 \cdot S^2 - 2629 \cdot S + 42,82 \quad (9)$$

$$R_p(S)|_{M=\frac{36g}{l}} = -2226 \cdot S^{1,401} + 30,6 \quad (10)$$

Finally, from Fig. 5c, we obtain the value of C:

$$C(S)|_{M=\frac{12g}{l}} = 29,34 \cdot \exp \left[ - \left( \frac{S-0,03959}{0,0252} \right)^2 \right] \quad (11)$$

$$C(S)|_{M=\frac{24g}{l}} = 36,16 \cdot \exp \left[ - \left( \frac{S-0,04043}{0,02884} \right)^2 \right] \quad (12)$$

$$C(S)|_{M=\frac{36g}{l}} = 472,6 \cdot S^{0,7062} - 5,526 \quad (13)$$

#### 4. Proposed Buck/Boost Converter and Control Strategy

##### A. Topology

To extract the CapMix energy and inject it into the grid, a bridgeless dual buck-boost converter is proposed (Fig. 6) that has very low losses, since the discharge from the cell to the grid goes through the input only once. Performance could be further improved by replacing the diodes with ZVS and ZCS MOSFETs. It operates in Boundary Conduction Mode (BCM) to achieve power factor correction on the grid side (by making the line current sinusoidal) and low current harmonics.

##### Operating Principle

For the analysis over a complete switching cycle BCM operation is assumed with identical PWM switching signals for S1 and S4, as are the signals for S2 and S3. This defines four modes of operation: two for the positive half cycle of the cell voltage, and two for the negative half cycle.

Mode I (Fig. 7a): Switches S1 and S4 are ON. L1 receives power from the input source. The coil current,  $i_{L1}$ , increases linearly from zero. The switches are turned on with zero current switching (ZCS). Diodes D1 and D2 are reverse biased. The output capacitor discharges and supplies power to the load.

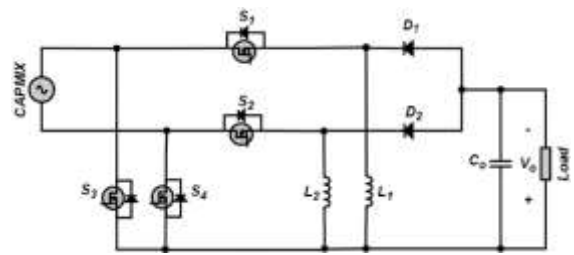


Fig. 6 Bridgeless Dual Buck/Boost Converter.

Mode II (Fig. 7b): Switches S1 and S4 are turned off.  $i_{L1}$  circulates freely through D1. The energy stored in L1 during Mode I is transferred to the load and also charges capacitor Co.  $i_{L1}$  decreases linearly until the coil is fully discharged. During this mode, there are switching losses when diode D1 turns on and MOSFET S1 turns off; these losses can be reduced by placing RC snubbers in parallel with the diodes and MOSFET switches.

Modes III and IV are respectively equivalent to modes I and II when the cell voltage is negative. It is enough to change the components S1+S4, D1 and L1 for S2+S3, D2 and L2.

It is also possible to operate the converter in Discontinuous Conduction Mode (DCM), which would add one more operating mode at the end of mode II and mode IV. During these periods, the coil current becomes zero. D1 and D2 turn off automatically at the end of modes II and IV respectively, the capacitor discharges through the load and thus provides power to it. The converter will return to modes I or III only when switches S1+S4 or S2+S3 are turned on. This behavior is shown in Fig. 8.

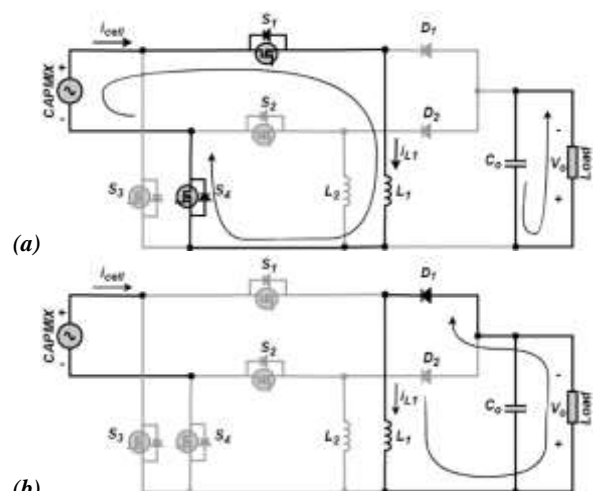


Fig. 7 Operating modes of the bridgeless dual buck/boost converter with positive input voltage: (a) Mode I; (b) Mode II.

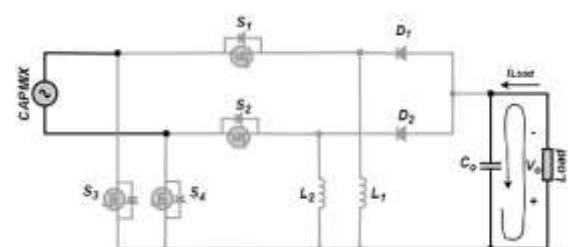


Fig. 8 Operating mode in DCM, both in the positive cycle of the input voltage and in the negative.

## B. Control Strategy

A hysteresis current control is proposed to fix the maximum and minimum values of the coil current. It does not require an external oscillator or sawtooth generator to operate and can provide fast response to transient events [9]. In this control technique (Fig. 9) the switch turns on when the coil current falls below the lower reference and turns off when it reaches the upper reference, resulting in variable frequency control [10]. It implements a polarity detector to detect the change in the sign of the cell voltage.

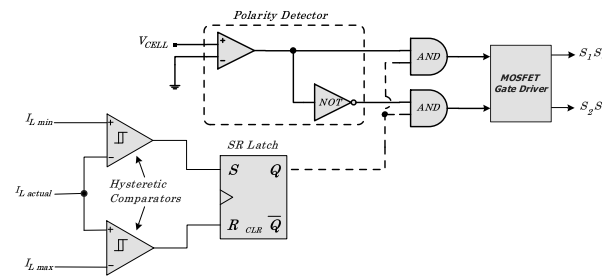


Fig. 9. Block diagram of current control by hysteresis.

## C. Transfer of Energy to the Grid

The dual buck-boost converter is configured to operate as a current source that must be injected to the AC grid. This is done by means of an inverter (see Fig. 10) that can be connected to the mains either directly or through a step-up transformer [11]. By monitoring the zero crossings of the mains voltage (either by Zero Cross Detection, ZCD, or by Phase Locked Loop, PLL [11]), it is possible to operate the MOSFETs of the inverter so that the current is always injected into the positive terminal of the AC mains.

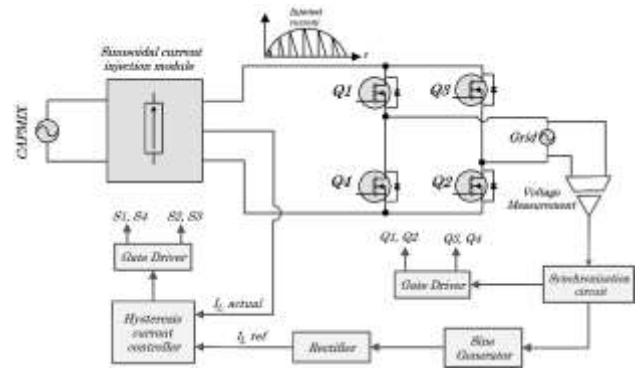


Fig. 10 Block diagram of the control system to inject energy from the CapMix cell into the network.

Additionally, if the reference for the inductor current is derived from the rectified mains voltage, the current injected by the dual buck-boost converter will have a sinusoidal shape in phase with the mains voltage, thus optimizing the energy transfer and the power factor of the system [12].

but this increase is more noticeable at very low voltages, when power transfer is lower and switching losses are higher. The maximum efficiency achieved is 70%

## 5. Simulation-Based Analysis

The behavior of the described converter has been simulated using the PLECS simulation software and representing the CapMix cell by the classic double-layer capacitor model. The simulations assume an initial voltage of 1V in the capacitor and a discharge of approximately 50%.

Fig. 13 shows the simulation of the complete discharge of a capacitive cell. If the cell voltage drops below 0.5V, the system loses control because the series resistance of the cell does not allow discharges at such a high current.

In the analysis carried out, specific instants of the AC mains voltage cycle are simulated by means of DC voltage sources with values between 5V and 310V. For each of these values, the influence of the reference in the hysteresis control (between 0.5A and 3A) is studied to analyze the transfer efficiency of the CapMix cell to the mains. The parameters of the CapMix cell used are those of a real cell available in the laboratory ( $C=1600F$ ,  $R_p=10\Omega$  and  $R_s=40m\Omega$ ). The first studies carried out determine the influence of the control current on the performance of the cell. Fig. 11 shows the current through the coil when the reference current is sinusoidal rectified with an amplitude of 1A. As indicated, the converter is working in BCM with hysteresis of the current. Note the variation in the switching frequency of the MOSFETs (1.8kHz - 12.5MHz). This frequency increases for low values of the current reference and so do switching losses. There are hysteresis control systems that produce a constant switching frequency [13].

## 6. Experimental Results

To validate the theoretical analysis, a preliminary prototype was built that allowed obtaining the waveforms advanced by the simulation. The input voltage was fixed at 2.5V. Fig. 14 shows the cell discharge and grid energy injection waveforms. The current reference is proportional to the mains voltage, so the injected current follows a sinusoidal evolution and provides power factor correction.

## 7. Conclusion

The present work explores the possibility of injecting the energy obtained in a capacitive mixing cell (CapMix) into the electrical AC mains by implementing a topology that

We see in Fig. 12 that, for any voltage value, increasing the coil current causes the efficiency of the system (cell + converter) to rise to a maximum (for  $I_L=1.2A$  in this case) after which the performance starts to drop. System performance is better for high values of the voltage cycle,

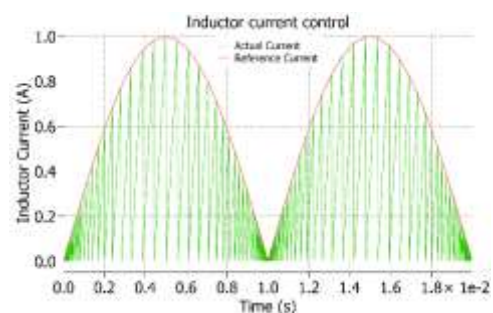


Fig. 11. Coil current with hysteresis control.

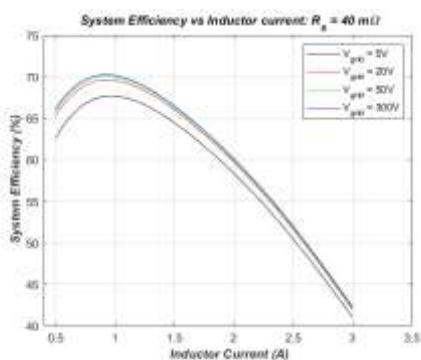


Fig. 12 System performance vs. reference current for various points of the network voltage.

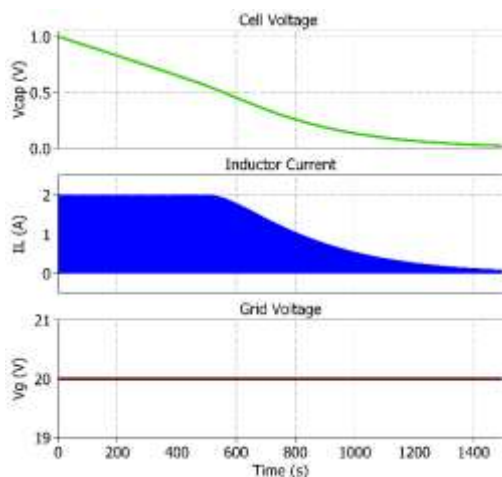


Fig. 13 Simulation of the current through the coil during a complete discharge cycle of the CapMix cell.

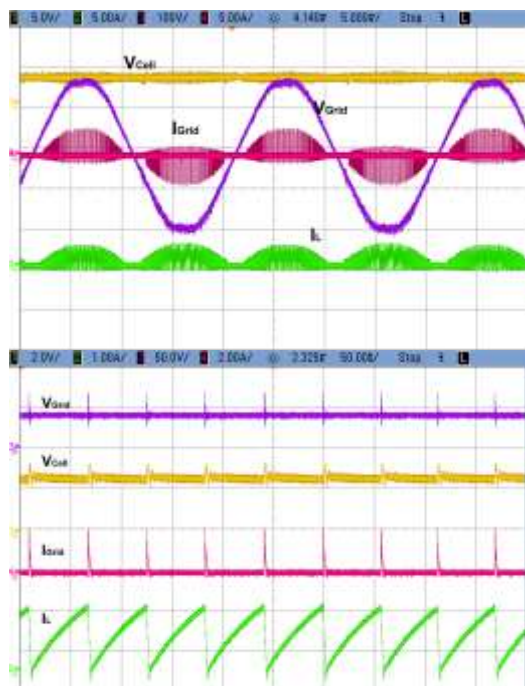


Fig. 14. Power injection in the grid ( $V_{Grid}=200V_{pk}$ ).  $I_L$ : Current through the coil;  $I_{Grid}$ : Current injected into the network.

injects current into the mains while providing power factor correction. Simulations determined that the maximum efficiency of this process is approximately 70%, and similar values were obtained in tests on prototypes. This value can

be increased by reducing the series resistance of the cell and the volume of water processed.

Although the characteristics of the CapMix cells still need to be improved, this work shows that this technology is an alternative to consider when generating renewable energy.

## Acknowledgement

This work has been funded by the Ministry of Science and Innovation of the Government of Spain through the ENAZUL project (reference PID2019-110971RB-I00).

## References

- [1] A. Qazi *et al.*, «Towards Sustainable Energy: A Systematic Review of Renewable Energy Sources, Technologies, and Public Opinions», *IEEE Access*, vol. 7, pp. 63837-63851, 2019, doi: [10.1109/ACCESS.2019.2906402](https://doi.org/10.1109/ACCESS.2019.2906402).
- [2] M. Simoncelli *et al.*, «Blue Energy and Desalination with Nanoporous Carbon Electrodes: Capacitance from Molecular Simulations to Continuous Models», *Phys. Rev. X*, vol. 8, n.º 2, p. 021024, abr. 2018, doi: [10.1103/PhysRevX.8.021024](https://doi.org/10.1103/PhysRevX.8.021024).
- [3] J. Ju, Y. Choi, S. Lee, y N. Jeong, «Comparison of fouling characteristics between reverse electro dialysis (RED) and pressure retarded osmosis (PRO)», *Desalination*, vol. 497, p. 114648, ene. 2021, doi: [10.1016/j.desal.2020.114648](https://doi.org/10.1016/j.desal.2020.114648).
- [4] M. Sharma, P. P. Das, A. Chakraborty, y M. K. Purkait, «Clean energy from salinity gradients using pressure retarded osmosis and reverse electro dialysis: A review», *Sustainable Energy Technologies and Assessments*, vol. 49, p. 101687, feb. 2022, doi: [10.1016/j.seta.2021.101687](https://doi.org/10.1016/j.seta.2021.101687).
- [5] J. Kim, J. Lee, y J. H. Kim, «Overview of pressure-retarded osmosis (PRO) process and hybrid application to sea water reverse osmosis process», *Desalination and Water Treatment*, vol. 43, n.º 1-3, pp. 193-200, abr. 2012, doi: [10.1080/19443994.2012.672170](https://doi.org/10.1080/19443994.2012.672170).
- [6] Sales, Bruno B., Fei Liu, Olivier Schaeztle, Cees JN Buisman, and Hubertus VM Hamelers. "Electrochemical characterization of a supercondensator flow cell for power production from salinity gradients." *Electrochimica acta* 86 (2012): 298-304.
- [7] D. Brogioli, R. Ziano, R. Rica, D. Salerno, O. Kozynchenko, H. Hamelers, and F. Mantegazza, "Exploiting the spontaneous potential of the electrodes used in the capacitive mixing technique for the extraction of energy from salinity difference," *Energy & environmental science*, vol. 5, no. 12, pp. 9870-9880, 2012.
- [8] Immanuel I. N. Jiya, N. Gurusinge, and R. Gouws, "Electrical circuit modelling of double layer condensadors for power electronics and energy storage applications: A review," *Electronics*, vol. 7, no. 11, p. 268, 2018.
- [9] A. M. Pernía, F. J. Alvarez-Gonzalez, M. A. J. Prieto, P. J. Villegas and F. Nuño, "New Control Strategy of an Up-Down Converter for Energy Recovery in a CDI Desalination System," in *IEEE Transactions on Power Electronics*, vol. 29, no. 7, pp. 3573-3581, July 2014, doi: [10.1109/TPEL.2013.2280814](https://doi.org/10.1109/TPEL.2013.2280814).
- [10] A. Pernía, F. J. Alvarez-González, J. Díaz, P. Villegas, and F. Nuño, "Optimum Peak Current Hysteresis Control for Energy Recovering Converter in CDI Desalination," *Energies*, vol. 7, no. 6, pp. 3823-3839, Jun. 2014.
- [11] B.-R. Lin and L.-A. Lin, "Implementation of an interleaved ac/dc converter with a high power factor," *Journal of Power Electronics*, vol. 12, no. 3, pp. 377-386, 2012.
- [12] C. Chandran and L. R. Chandran, "Two switch buck boost converter for power factor correction," in *2015 International Conference on Technological Advancements in Power and Energy (TAP Energy)*. IEEE, 2015, pp. 454-459.
- [13] M. Biswal, "Control techniques for dc-dc buck converter with improved performance," Master's thesis, National Institute of Technology Rourkela, 2011.